frontiers | Frontiers in Environmental Science

TYPE Original Research
PUBLISHED 26 September 2024
DOI 10.3389/fenvs.2024.1472175

OPEN ACCESS

EDITED BY
Longlei Li,
Cornell University, United States

REVIEWED BY
Aleksandar Valjarević,
University of Belgrade, Serbia
Zhishan An,
Chinese Academy of Sciences (CAS), China

*CORRESPONDENCE
Long Li,
lilongdhr@126.com

RECEIVED 29 July 2024
ACCEPTED 02 September 2024
PUBLISHED 26 September 2024

CITATION
Zhang Y, Li L, Liu L, Zhang S, Zhao W, Ren Y and Yang Y (2024) Spatiotemporal variation and driving force of gully erosion in the Pisha sandstone area.
Front. Environ. Sci. 12:1472175.
doi: 10.3389/fenvs.2024.1472175

Spatiotemporal variation and driving force of gully erosion in the Pisha sandstone area

Yu Zhang[1], Long Li[1,2]*, Linfu Liu[1], Shangxuan Zhang[1], Wenzhuo Zhao[1], Yanan Ren[1] and Yue Yang[1]

[1]College of Desert Control, Science, and Engineering, Inner Mongolia Agricultural University, Hohhot, China, [2]Key Laboratory of Desert Ecosystem Protection and Restoration, State Forestry Administration, Hohhot, China

The experiment was conducted on gully slopes with slopes ranging from 80° to 90° to investigate the relationship between erosion rates, spatial and temporal changes in microtopography, and drivers of erosion on gully slopes in different seasons. To precisely characterize the microtopography of slopes where debris slides occur, we used the RIEGL VZ-400 3D laser scanner to scan the observation site and acquire point cloud data on the slope's microtopography. Using the "data conversion module" of ArcGIS software, the point cloud data were transformed into raster data. Through the "3D analysis," "hydrological analysis," and "grid calculator" modules, the basic microgeomorphological indicators were extracted from the gully slope grid data, and the erosion rate and microterrain evolution mechanism of the gully slope in different seasons were also determined. The results revealed the following: (1) in the Pisha sandstone area, erosion was relatively strong in the first quarter, with 65% of the area being eroded. The average erosion rates over the four quarters followed the order of first quarter > fourth quarter > second quarter > third quarter, from fastest to slowest. (2) As the soil on the gully slope thawed, melt water increased soil moisture. This phenomenon sharply increased surface roughness in the first quarter. The correlation coefficients between the erosion rate and temperature in the first and fourth quarters were 0.75 and 0.82, respectively. Temperature mainly affected the erosion rate through surface roughness. The direct path coefficient of this effect was 0.72. (3) In the first and fourth quarters, temperature and wind speed were the main factors influencing the erosion rate; the relationship between surface roughness and other factors was evident, making surface roughness the best topographic factor for assessing slope erosion in the Pisha sandstone area. The results of this study aim to provide theoretical references for understanding the gravity erosion mechanism of gully slopes in the Pisha sandstone area and contribute to the high-quality development of the Yellow River Basin.

KEYWORDS

debris slide, erosion rate, microgeomorphology, Pisha sandstone, quarterly, ArcGIS

1 Introduction

A debris slide is a phenomenon where soil and rocks on rock walls and steep slopes roll or slide down under the action of gravity to form steep cones. It is caused by the shrinkage induced by the temperature difference between winter and spring and physical weathering. This phenomenon is ubiquitous in the vicinity of the Yellow River Basin and mainly leads to

the formation of laterite slippery surfaces. Under the long-term influence of debris slides, typical gravity erosion is encountered in the Pisha sandstone area bordering Shanxi, Shaanxi, and Inner Mongolia, China, and soil on the gully slopes is constantly eroded, transported, and accumulated, resulting in different changes in gully slopes on different spatial and temporal scales. This work aims to address the research gaps in debris slide erosion by focusing on the erosion rates and microgeomorphological evolution mechanisms of gully slopes in the Pisha sandstone area.

The Pisha sandstone mainly refers to a loose rock layer consisting of thick sandstone, sand shale, and muddy sandstone, formed during the Permian, Triassic, Jurassic, and Cretaceous periods of the Paleozoic era. It mainly consists of a parent material layer, a grayish-white calcareous layer, and a humus layer, all of which have a poor ability to retain fertilizer and water. The physicochemical properties of the rock and soil are the decisive factors affecting the debris slides (Yuhong, 2018). When the minerals within the rock and soil body exhibit properties such as water expansion, dehydration, and cracking, the debris slide is more likely to occur (Gao et al., 2020). For example, the Pisha sandstone mineral composition is mainly quartz, feldspar, montmorillonite, and calcite (the average content of more than 50%), in which feldspar and montmorillonite are easily weathered, and the average content of the feldspar and montmorillonite is more than 50%. Montmorillonite expands when it comes into contact with water, and calcite easily decomposes, which has a great impact on the corrosion resistance of the Pisha sandstone by not only reducing the physical and mechanical properties of the rock (Ye et al., 2006) but also causing easy weathering and the easy loss of nutrients (Yan et al., 2016). The process of water erosion often shows obvious gravity erosion characteristics (Yin et al., 2021), making the lagging and lagoonal erosion phenomena in the Pisha sandstone area highly likely to occur. Therefore, the different compositions of rock and soil minerals, water content, fissure characteristics, and the stratigraphic combination of the same lithology and interbedding, etc., determine the different scales and rates of debris slide erosion. In the Pisha sandstone area, the chemical composition of the Pisha sandstone can cause significant changes in cohesion (Ye et al., 2008); even different colors of the Pisha sandstone show varying resistance to water erosion (Wen-Yi et al., 2018). Meanwhile, slope gradient and height are the main factors affecting gravity erosion. In a study of the Loess Plateau, bordering Shanxi, Jin, Shaanxi, and Mongolia, the influence of geomorphological factors on gravity erosion was analyzed, and the results showed that steep slopes in the Loess Liangxuan hilly area are prone to landslides (Matsunaga and Zhimao, 2007).

The Pisha sandstone area, a typical concentrated source area of coarse sand in the Yellow River Basin, has a low degree of diagenesis and weak corrosion resistance, resulting in strong gully erosion. In the Yellow River Basin, soil erosion affects not only the water quality and ecological environment but also the biogeochemical cycle. Current climate change suggests that rainfall conditions may increase the risk of erosion (Yousefi et al., 2022). Related studies have shown that the effects of climate change on soil erosion were explored based on the random forest regression model (Liu et al., 2024). The RUSLE model and geodetector method are used to provide a reference for the study of integrated soil erosion control and ecological environment quality improvement in watersheds in the Loess Plateau region (Zhang et al., 2023). GIS and other tools are used to analyze the main factors of linear erosion and surface erosion and predict future landslides (Valjarević et al., 2015). Regional and seasonal climate change is an important factor in triggering debris slides (Wang et al., 2019), and rainfall, as the main power source of soil erosion (Zhu et al., 2019), exerts a great influence on the debris slide process (Zhang and Kai, 2021). Debris slides mostly occur in the rainy season, and the scale of occurrence is positively correlated with rainfall (Zhu et al., 2017; Yujie et al., 2021). However, rainfall does not directly influence the debris slide process, which is also related to rainfall intensity (Wu, 2020). With the increase in rainfall intensity, the cumulative runoff volume, cumulative sand production, and the rate of infiltration gradually increase (Chai et al., 2019), and the rainfall excitation that causes surface runoff is also an important factor and additional driver for inducing large amounts of soil loss (Wei et al., 2012). Changes in temperature and humidity also have an impact on debris slide; for example, with the change in temperature, the volume change in the Pisha sandstone freezing and thawing leads to a corresponding change in the characteristics of the soil skeleton (Chen et al., 2016).

Therefore, the interaction between erosion and climate change (Li and H, 2016) aggravates the problem of ecological security in the Pisha sandstone area. Climate plays an important role in the occurrence and behavior of ooze erosion. Wind is an important force shaping landforms in arid and semiarid areas. Wind can directly affect the transformation and transmission of erosion materials (Liu et al., 2022). Temperature is the main cause of gully erosion and affects the freezing and melting of gully soil in the fourth and first quarters, respectively (Barnes and Luffman, 2016). It loosens soil and aggravates erosion. The erosion of gully slopes by rainfall mainly occurs in the rainy season and can quickly remove soil when gully slopes are drained (Ryan and Kate, 2021). Solar radiation can cause the evaporation of soil moisture during debris slide erosion and aggravate gully slope erosion (Fang and Guo, 2015). The superposition of wind speed, temperature, rainfall, and solar radiation on an area of gully slope erosion is more severe than that on an area undergoing a single type of erosion. Research on gully slope erosion under meteorological factors in different quarters, especially on fine spatial and temporal scales, is lacking. The composite effect of meteorological factors is a root cause of ooze erosion. The climate of the Pisha sandstone area must be studied to provide a reference for soil erosion control.

The fluctuations in microgeomorphology and yield of accumulation caused by debris slides are due to gully slope retreat, which is a crucial phenomenon for various geological disasters and erosion studies. Although numerous studies have been conducted on the gravity erosion of gully slopes around the world in recent years, most of them focused on landslides, collapses, and debris flows (Yu et al., 2016; Liu et al., 2020; Zou et al., 2023; Zhu et al., 2021; Lyu et al., 2017). The debris slide erosion of the gully has received little attention. The rate of ooze erosion in different quarters helps elucidate the response of microtopographical changes to climate forcing. When the soil of a gully slope is constantly eroded, microtopography also evolves, and the fluctuation in microtopography is the most direct embodiment of the results of gully slope erosion. In addition, due to the rapid occurrence of slippage and low single-erosion volume, erosion is difficult to detect.

This situation accounts for the scarcity of current research on slope slippage in the Yellow River area. In view of the lack of a systematic and comprehensive understanding of the development mechanism of ooze erosion in the Pisha sandstone area, a comprehensive spatial and temporal observation of the changes in the debris slide erosion–transport–accumulation of gully slopes in the Pisha sandstone area is urgently needed to reveal the ooze problem of gully slope systems in the Yellow River Basin, Inner Mongolia.

The techniques used for gully slope scanning mainly include LiDAR (Bi et al., 2021) and UAV monitoring (Cndido et al., 2020). The 2D LiDAR has low accuracy and lacks height information for 2D imaging. The latter characteristic precludes imaging. UAV mapping requires good weather conditions. Otherwise, meteorological factors, such as wind speed and rain, may affect the flight and shooting of UAVs and may have a negative effect on data. In lieu of 2D LiDAR and drone monitoring, our research used a three-dimensional (3D) laser scanner to monitor gully slope erosion in detail. High-precision 3D laser scanning technology (Wulf and Wagner, 2003) and computational resources (Mostafa, 2015) can monitor the temporal and spatial changes in gully slope surfaces. ArcGIS was used to quantify the erosion–transport–accumulation in debris slides, starting from single erosion to deposit formation. Given that data monitoring and collection were repeated on-site every quarter, this approach is cost-effective and can describe the characteristics of gully slope erosion in detail.

The Yellow River Basin had a total erosion area of 21 × 108 t from 1985 to 2020 (Ni et al., 2008) and an average erosion modulus of 1,160.97 t/km^{-2}/yr^{-1} (Guo et al., 2024). In the Yellow River Basin, the Jiziwan area is a key site for ecological protection and high-quality development. In the past, most research on the sediment source area of the Yellow River Basin was based on various deserts in China, such as the Ulan Buh (Li M et al., 2023), Kubuqi (Du He et al., 2017), and Tengger deserts (Li Y et al., 2023). Only a few reports on ooze erosion in the Pisha sandstone area of the Yellow River in Inner Mongolia exist. Therefore, this work used ArcGIS and 3D scanning and positioning monitoring technology in a gully slope field along with HOBO meteorological station data and 3D laser scanning point cloud data to focus on the spatial distribution and process of ooze erosion in the Pisha sandstone area. Moreover, it discussed the mechanism underlying the influence of meteorological and microgeomorphological factors on ooze erosion rates in each quarter. This study considered two scientific questions: (1) how do seasonal changes affect the spatial and temporal heterogeneity of ooze erosion? (2) What is the relationship between quarterly changes, gully erosion rates, and microgeomorphological factors? This study clarified the characteristics of ooze erosion in response to seasonal changes and provided new insights for soil and water conservation work and planning in the Yellow River Basin.

2 Materials and methods

2.1 Overview of the study area

The study area is located in the Baojiagou River Basin (110°31–110°35′E, 39°46′–39°48′N) in Zhungeer Banner, Ordos City, Inner Mongolia (Figure 1). The basin area is 12.67 km^2. The study area has a temperate continental climate, an average altitude of 1,200 m, and abundant light resources. Its annual sunshine hours are 3,100–3,200 h, its annual sunshine rate exceeds 70%, its annual average temperature is 7.2°C, and its average frost-free period is 135 days. Its average annual rainfall is 400 mm. Rainfall in the study area mainly occurs from June to August. In the study area, the average annual rainfall in summer is 256 mm, which accounts for 4.1% of the total annual rainfall.

The soil bedrock is composed of feldspathic sandstone, and part of the rock interbed is composed of sandstone, sand shale, and argillaceous sandstone. The main minerals of gray–white and purple–red sandstone are quartz, calcium montmorillonite, and calcite (Ye et al., 2007), and the mineral compositions of Pisha sandstone with different lithologies differ (Table 1). Due to the different mineral compositions of different lithologies, rocks with large porosity provide the basis for the development of gully slope erosion (Ma et al., 2020). The test results show that purple has a larger capacity and less porosity. This indicates that purple is more compact than the sandy sandstone structure and has weak water permeability. The gray–white porosity is larger than that of the sandy sandstone, indicating that the structure and good water permeability are loose, which creates favorable internal conditions for gully slope erosion. The sandy sandstone belongs to the purple and gray rock period. Thus, the gray–white sandy sandstone is more susceptible to erosion (Table 2). The shear strength characteristic of the rock is generally characterized by cohesion (c) and internal friction angle (φ). The highest adhesion of the purple Pisha sandstone is 203.45 kpa, and the lowest adhesion of the gray Pisha sandstone is 184.9 kpa. The shear strength of Pisha sandstone, when compared between the different colors, is in the order (highest to lowest): purple–red sandstone > mixed-color sandstone > gray–white sandstone (Table 3). Most gully slopes have almost no vegetation and are covered by a thin layer of loess or floating sand, generally 10–150-cm thick. Given the large differences in mineral and cement compositions, the average total erosion modulus in the Pisha sandstone area is as high as 44,570 t/km^2/y^{-1}. Gravity erosion accounts for 30.6% of the average total erosion in the area, and the soil loss rate is approximately 1.5 × 104 t/km^{-2}/y^{-1}. The region transports 100 million tons of sediment to the Yellow River every year and is, therefore, a main source of coarse sediment in the Yellow River Basin (Yang et al., 2019).

2.2 Experimental design

2.2.1 Sample selection and establishment

The experiment began in 2023. The research plot was a part of the typical bare Pisha sandstone area. In accordance with the actual terrain conditions, a bare sunny slope with a gradient of 80°–90° (Figure 2) was selected as the research object. The purpose of this study was to monitor the erosion of the selected gully slope in each quarter. January–March, April–June, July–September, and October–December were regarded as the first, second, third, and fourth quarters, respectively.

The HOBO weather station was set up for field monitoring. A sample rope was used to pull out two sample lines perpendicular to

TABLE 1 Characteristic values of the mineral compositions of Pisha sandstone.

Project	Gray–white sandstone		Purple–red sandstone		Gray–white and purple–red banded sandstone	
	Average content	Standard deviation	Average content	Standard deviation	Average content	Standard deviation
Quartz	50.5	11.3	50.8	8.2	42.5	7.5
Calcium montmorillonite	20.0	7.0	15.8	4.8	24.0	1.0
Calcite	11.0	9.0	12.0	7.2	1.0	1.0

TABLE 2 Basic physical properties of different colored Pisha sandstone.

Pisha sandstone property	Unit weight/ ($g{\cdot}cm^{-3}$)	Soil moisture content/(%)	Total porosity/ (%)	Capillary porosity/ (%)	Noncapillary porosity/(%)
Purple–red Pisha sandstone	1.507	7.984	24.740	18.432	6.308
Gray–white Pisha sandstone	1.401	8.687	30.991	24.296	6.564
Gray–white and purple–red banded sandstone	1.474	8.329	26.422	19.646	6.776

TABLE 3 Disintegrating process of different colored Pisha sandstone.

	Gray–white sandstone	Gray–white and purple–red banded sandstone	Purple–red sandstone
Cohesion	c = 184.9	c = 195.2	c = 203.45
Internal friction angle	∅ = 32.77	∅ = 33.88	∅ = 41.52

the gully slope from the top to the bottom of the gully to avoid disturbing the original gully slope and ensure the integrity of the sample plot. The distance between the two sample lines was 5 m, and an observation plot with a width of 5 m was established with the sample line as the boundary. A fixed cement pile was arranged at the bottom and left and right sides of the gully slope as the station for data scanning to ensure the consistency of each scanning condition, and 5–8 fixed reference points were selected as the splicing reference points after scanning data. Finally, a 3D laser scanner was fixed with a tripod (100 cm from the ground height) at the scanning position and height of the gully slope for a comprehensive scan to obtain microgeomorphological point cloud data. The 3D laser scanner used in the test is RIEGL VZ-400, which is characterized by high speed without contact and high accuracy. Its measurement frequency can reach 1,200 khz, the scanning accuracy is ±2 mm in a 100-m range, the scanning distance is 600 m (90% reflectivity), and the scanning range is 100° (vertical) × 360° (horizontal). In addition, the 3D laser scanner applies waveform digitization and online waveform analysis technology to deliver up to 300,000 fine laser beams per second, providing high-resolution digitization and real-time waveform analysis. The 3D laser scanner can emit up to 300,000 fine laser beams per second, providing an angular resolution of up to 0.0005. The elevation point cloud data of the gully slope were collected and converted into raster data by using the data conversion module of the ArcGIS software platform. The accuracy of the point cloud data can reach 2.0 mm in the horizontal direction and 1.5 mm in the vertical direction. MDEM with a resolution of 2 mm × 2 mm was generated after conversion into raster data for the determination of the retreat speed, erosion intensity classification, and spatial pattern of gully erosion.

2.2.2 Observation of gully slope erosion

The fluctuations in the microgeomorphology of the gully slope erosion interface are the most direct manifestations of erosion. Therefore, this study observed the gully slope retreat at the end of each month in 2023 to reveal the process of gully slope retreat. An observation and collection area for slope bottom deposits was established, with dimensions of 2.5 m (width) × 5 m (length) at the bottom of the observation plot, and a 3D laser scanner was used to scan the microgeomorphological point cloud data of the gully slope.

The MDEM of two adjacent observation gully slopes was generated in ArcGIS software. The MDEM difference between slopes can quantitatively describe the changes in gully slope retreat. The slope DEM was constructed after the end of the scan. First, the scanned point cloud data were processed using RiSCAN PRO software for noise reduction and splicing, the 3D point coordinate attributes were set, and the ".txt" point coordinate data were exported. Then, the 3D point coordinate data were imported into ArcGIS software for spatial calibration. The calibrated point cloud data were used for generating the TIN vector data, and then, the TIN vector data were converted into a

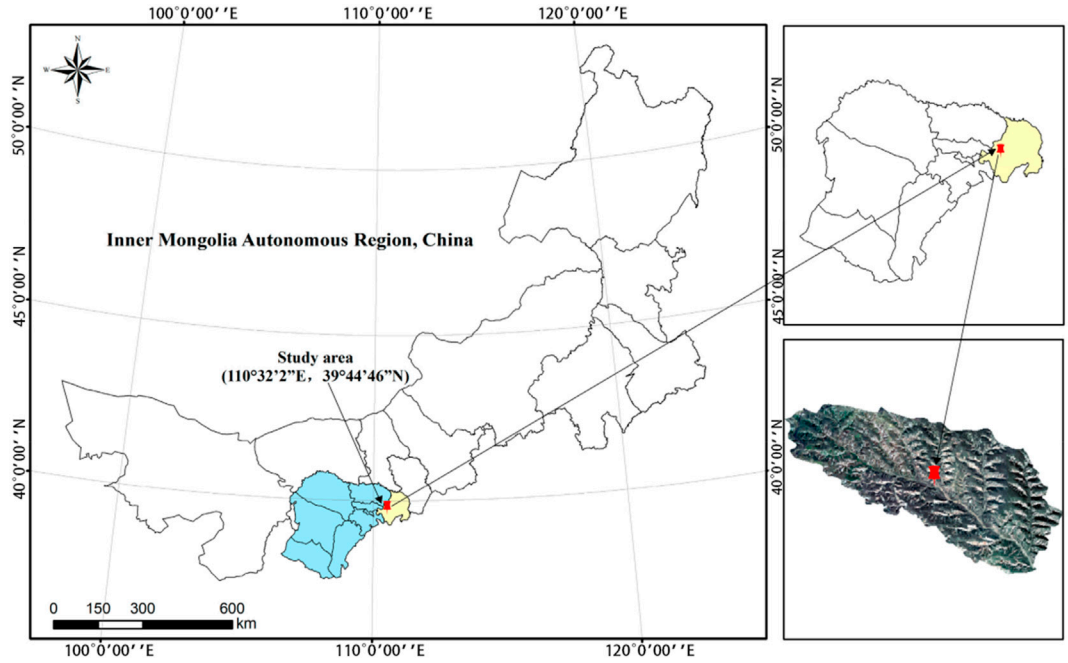

FIGURE 1
Map of the study area

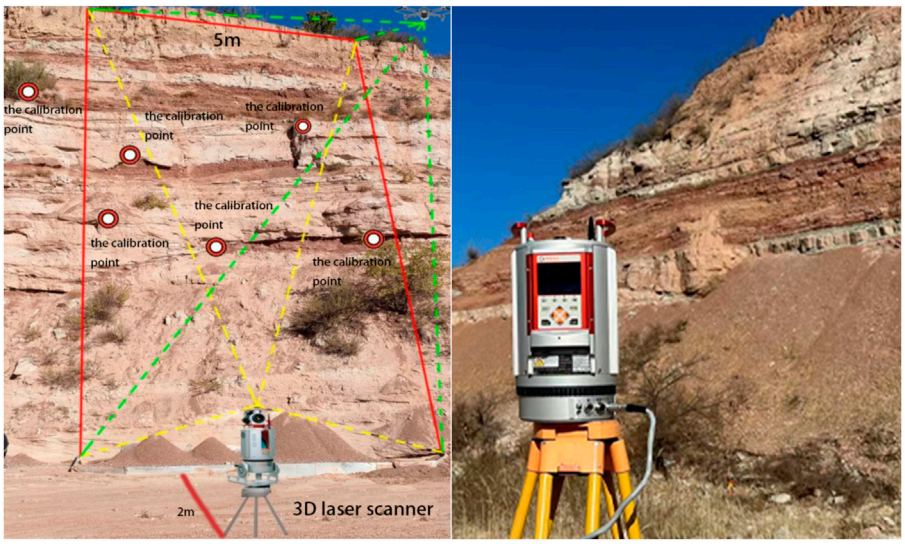

FIGURE 2
Position of a sample plot.

high-precision ground surface digital elevation model (MDEM, with an accuracy of 2°mm × 2 mm) using the conversion tool. The previous microgeomorphological model (before MDEM) was subtracted from the later microgeomorphological model (after MDEM). If ΔMDEM = (before MDEM) − (after MDEM) < 0, then the corresponding area is the erosion area, that is, the gully slope retreat area. If ΔMDEM = (before MDEM) − (after MDEM) > 0, then the corresponding area is the accumulation area, that is, the corresponding area plays an interception or retention role in drainage and the eroded debris accumulates on the gully slope. If ΔMDEM = (before MDEM) − (after MDEM) = 0, then the relative position of the gully slope in the non-erosion area does not change.

2.2.3 Index calculation

The three-dimensional data are imported into ArcGIS software to generate the height data model of gully slope microtopography.

(1) Erosion area (TEA)

$$TEA = n \times A.$$

In the formula, n represents the number of grids in the erosion area and A represents the area of the statistical unit grid.

(2) Erosion volume (TVA)

$$TVA = S \times H.$$

In the formula, S represents the area of erosion area and H represents the average elevation.

(3) Corrosion rate (V)

$$\text{Erosion per unit time per unit area.}$$

(4) Microslope (S)

The inclination of the local surface at this point is extracted using the slope function of ArcGIS.

(5) Surface roughness (R)

Ground roughness refers to the ratio of the earth's surface area to its projected area, calculated using map algebra in a specific area based on the slope, which can intuitively reflect surface fluctuation and erosion in that area. The formula is as follows:

$$R = 1/\mathrm{COS}([\text{Slope of DEM}] \times \pi/180.$$

In the formula, R represents the surface roughness of a specific area, [Slope of DEM] refers to the DEM slope of a certain layer, and π generally takes the value of 3.14159.

(6) Relief degree of land surface (RA)

Surface undulation refers to the height difference between the lowest and highest altitudes in a certain area, which can directly reflect the fluctuation in the surface in the process of soil erosion. It is a macroscopic index of regional topography. The formula is as follows:

$$RA_i = H_{max} - H_{min}..$$

In the formula, RA_i represents the relief amplitude of the terrain in a certain area, H_{max} represents the height value of the highest point in the range, H_{min} represents the lowest height value in the range, and i represents the symbol of a specific area.

(7) Surface cutting degree (SI)

The cutting degree refers to the difference between the average altitude and the lowest altitude in the vicinity of a certain point, which can directly reflect the situation of surface erosion and cutting. The formula is as follows:

$$SI_i = H_{mean} - H_{min}..$$

In the formula, SI_i represents the surface cutting depth at a certain point in the area, H_{mean} represents the average height value in the area, and H_{min} represents the lowest height value in the area.

RiSCAN PRO and ArcGIS 10.6 software applications were used to calculate the amount of erosion and topographic factors. R language, SPSS Amos, and Excel software programs were used to process and analyze the data, and Origin 2019 software was used to make charts.

3 Results and analysis

3.1 Characteristics of gully slope erosion intensity

The average elevation changes in the surface of the Pisha sandstone gully slope in each quarter (Figure 3) were analyzed in accordance with the size and spatial location of ΔMDEM, and the results were used to classify gully slope erosion intensity. Table 4 shows that from the first to the second quarter, the deposition area increased by 35%, whereas the erosion area decreased by 12%. In the first and fourth quarters, the erosion area accounted for the largest proportion, that is, 65% and 58%, respectively. The total erosion area accounted for 9.6337 and 8.5352 m^2, respectively. The erosion area in the third quarter was the smallest, accounting for 42%, and the sedimentary area in the third quarter was the largest, accounting for 8.6336 m^2. In the four quarters, the gully slope concentrated at erosion depth < −3 cm. Therefore, erosion in the sandstone area is intense.

3.2 Characteristics of the variations in the erosion rates of the gully slope

Overall, in all four quarters, the top of the gully slope showed intense erosion fluctuation, whereas the bottom of the gully slope experienced sedimentation. Figure 4 shows that the average erosion rate decreased by 22.2% from 0.2634 $t/m^2 \cdot m$ in the first quarter to 0.2049 $t/m^2 \cdot m$ in the second quarter. The average erosion rate decreased by 32.3% from 0.2049 $t/m^2 \cdot m$ in the second quarter to 0.1388 $t/m^2 \cdot m$ in the third quarter. The average erosion rate increased by 38.1% from 0.1388 $t/m^2 \cdot m$ in the third quarter to 0.2242 $t/m^2 \cdot m$ in the fourth quarter. The average erosion rates of the four quarters followed the order of first quarter > fourth quarter > second quarter > third quarter, from fastest to slowest. The average erosion volume in the first quarter was 27.5, 88.1, and 16.6 times that in the second, third, and fourth quarters, respectively. Table 5 shows that erosion amount per unit area in the four quarters was between 0.0429 and 0.0914 m^3/m^2. The average erosion amount per unit area in the first quarter was the highest, at 0.0871 m^3/m^2, whereas the erosion amount per unit area in the third quarter was the lowest, at 0.0581 m^3/m^2.

3.3 Variation characteristics of gully slope microtopography

Gully slope erosion is accompanied by changes in microtopography, which reflect the characteristics of erosion. In this study, the characteristics of four microgeomorphological indexes of gully slopes, namely, microslope, surface roughness, surface cut, and surface relief were analyzed to reveal the law of microgeomorphological changes in the Pisha sandstone area. The results are shown in Table 6. The microslope, surface undulation,

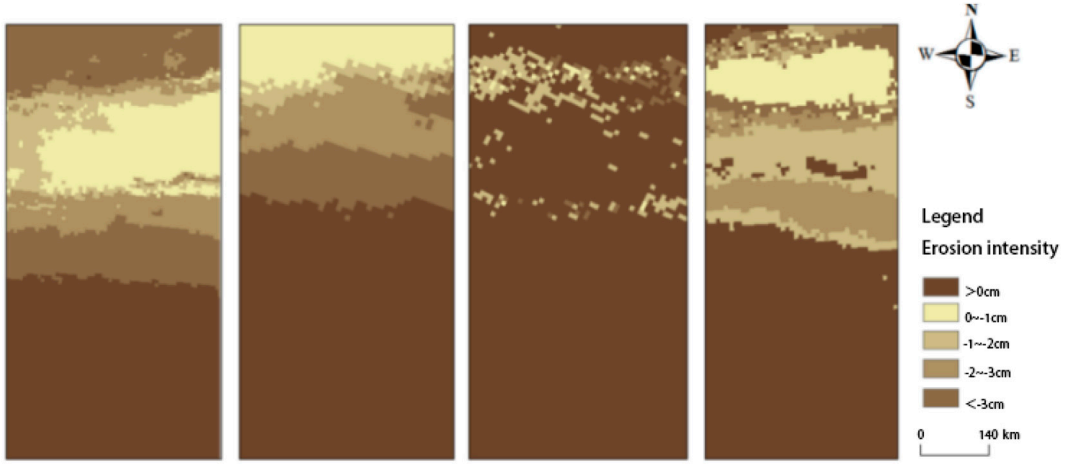

FIGURE 3
Slope erosion intensity in each quarter.

TABLE 4 Summary of the changes in digital elevation models after slope erosion in each quarter.

Quarter	Observation date	Total sedimentary area (m^2)	Erosion intensity				Total erosion area (m^2)	Erosion area (%)
			0~−1 cm	−1~−2 cm	−2~−3 cm	<−3 cm		
First quarter	2024.1.20	5.1453	1.0453	1.7832	2.4710	4.3342	9.6337	65
Second quarter	2023.4.22	6.9353	0.5920	1.4231	2.7040	3.7546	7.8437	53
Third quarter	2023.7.21	8.6336	0.6700	0.9931	1.3172	3.1651	6.1454	42
Fourth quarter	2023.12.22	6.2438	1.8291	1.3532	1.6938	3.6591	8.5352	58

Erosion is divided into five levels: >0 cm is sedimentation; 0–1 cm is slight erosion; −1–−2 cm is mild erosion; −2–−3 cm is moderate erosion; and <−3 cm is strong erosion (Li et al., 2021).

TABLE 5 Basic characteristics of gully and slope erosion in different seasons.

Quarter	Observation date	Average depth DEM/m	Erosion area (m^2)
First quarter	2024.1.20	0.0911	10.0293
	2024.2.21	0.0896	9.2381
	2024.3.21	0.0905	9.6337
Second quarter	2023.4.22	0.0849	7.6734
	2023.5.20	0.0893	8.0138
	2023.6.22	0.0871	7.8439
Third quarter	2023.7.20	0.0724	5.9216
	2023.8.23	0.0782	6.3692
	2023.9.20	0.0753	6.1454
Fourth quarter	2023.10.22	0.0911	8.5685
	2023.11.21	0.0839	8.5019
	2023.12.20	0.0875	8.5352

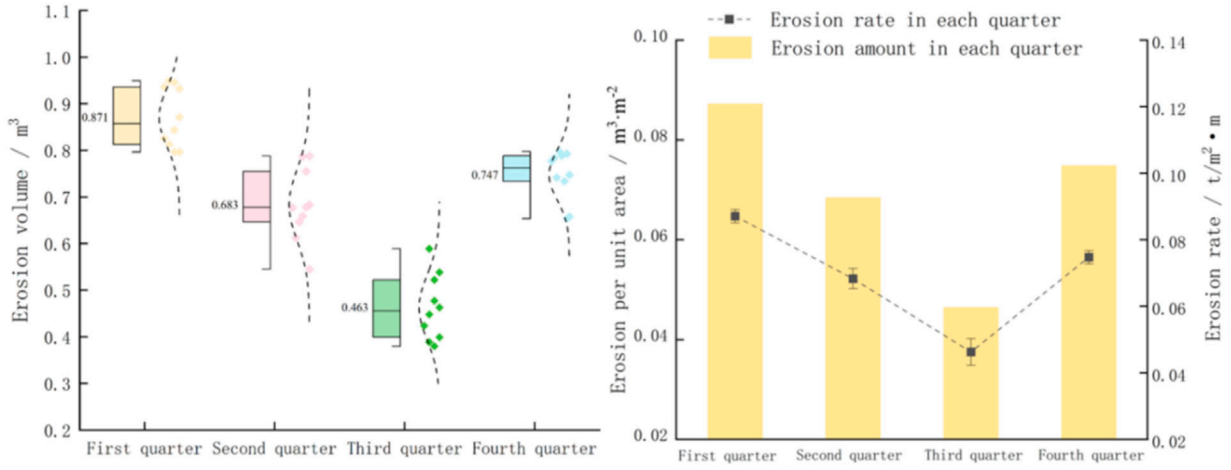

FIGURE 4
Basic characteristics of slope erosion in each quarter.

TABLE 6 Characteristics of microtopographical changes in each quarter.

Quarter	Microslope (°)	Relief degree (m)	Cutting degree (m)	Roughness degree (m)
First quarter	44.30	0.2149	0.1475	2.6906
Second quarter	42.6172	0.2058	0.1307	1.7466
Third quarter	42.5389	0.1902	0.1177	1.7415
Fourth quarter	43.1607	0.2431	0.1581	1.7189

and surface cutting degree in the second quarter reduced by 4.0%, 4.2%, and 12.9%, respectively, compared with those in the first quarter. The microslope, surface undulation, and surface cutting degree decreased by 0.2%, 7.6%, and 10.0%, respectively, from the second to the third quarter. The microslope, surface relief, and surface cutting degree in the fourth quarter increased by 1%, 5.3%, and 25.6%, respectively, relative to those in the third quarter.

The changes in the above four microtopographical factors showed that topographical factors (except surface roughness) decreased in the second and third quarters. Among the four microgeomorphological indexes of the gully slope, the surface cutting degree showed the most discernible change, increasing from 1.6% to 36.1%. The topographical factors of the gully slope changed drastically from the first to the second quarter. Gully slope ooze in the Pisha sandstone area exhibited spatial differences in each quarter, and the location of the gully slope had an effect on erosion (Figure 5). The fluctuation in erosion at the top of the gully slope in the four-quarters was the most intense, followed by that at the middle of the gully slope, and that at the bottom of the gully slope showed low intensity.

3.4 Characteristics of the variations in the meteorological factors of gully slopes

Figure 6 shows that rainfall increased from the first to the third quarter and decreased from the third to the fourth quarter. The average values of rainfall in the first, second, third, and fourth quarters were 3.15, 399.22, 139.94, and 0.13 mm, respectively. The average temperatures in the first and fourth quarters were low and were −0.11°C and 4.74°C, respectively. Temperature exhibited the following variation: temperature increased first from the first to the second quarter and then gradually decreased from the second quarter to the fourth quarter. The amplitudes of temperature from the first to the second quarter and the third to the fourth quarter were large and were 99.5% and 78.3%, respectively. The average solar radiation reached the highest value of 234.6 W/m^2 in the second quarter and the lowest value of 83.00 W/m^2 in the first quarter. Wind speed fluctuated in the first and fourth quarters, and the average wind speed in the fourth quarter was the largest, at 5.17 m/s.

3.5 Relationship among meteorological factors, erosion rates, and microtopographies of Pisha sandstone gully slopes

Given that the erosion rate of each quarter differed, the correlation between the erosion rates and microgeomorphologies of the gully slope was determined based on the data from all four quarters. Different colors in Figure 7 represent different levels. A dark color is indicative of high significance. A large circular area indicates a high correlation coefficient. Red represents a positive correlation, and blue represents a negative correlation. Figure 7

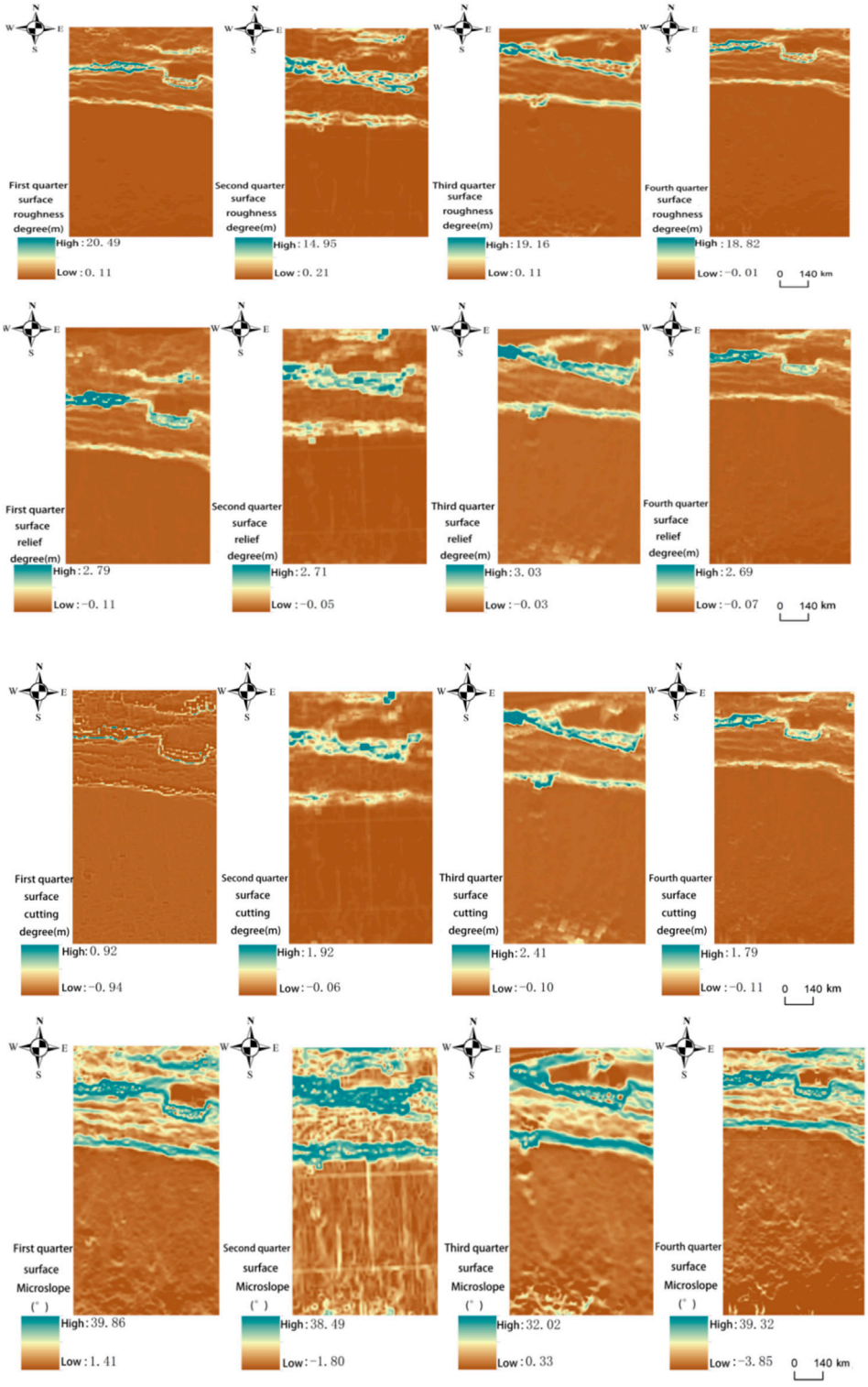

FIGURE 5
Changes in terrain factors in each quarter.

shows that in the first quarter, temperature had the greatest influence on the microslope, surface roughness, surface cutting degree, surface undulation, and erosion rate, with correlation coefficients of 0.30, 0.87, 0.83, 0.80, and 0.75, respectively. The correlation between the erosion rate and surface relief was the highest, with a value of 0.97. In the second quarter, meteorological factors had a minimal effect on microgeomorphological factors and erosion rates, and the temperature was negatively correlated with surface relief with a correlation coefficient of −0.12. The surface cutting degree was

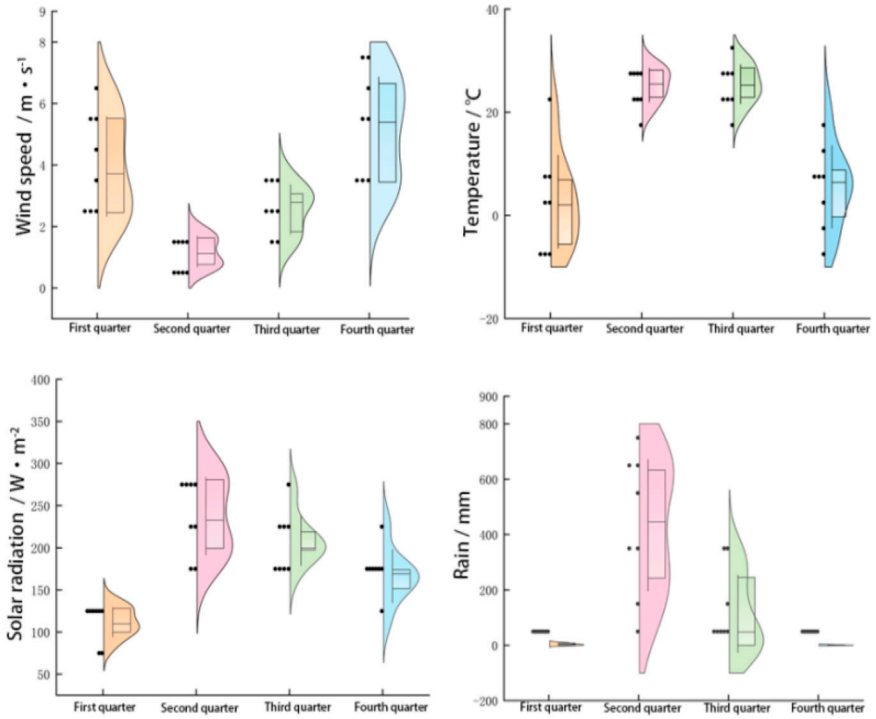

FIGURE 6
Quarterly meteorological data.

positively correlated with surface roughness with a correlation coefficient of 0.80. In the third quarter, wind speed and solar radiation had a strong correlation with microtopographical factors, whereas temperature and rainfall had a weak correlation with microtopographical factors. In the fourth quarter, meteorological factors had a strong correlation with microtopographical factors and erosion rate. Among these factors, temperature had a strong influence on the microslope, surface roughness, surface cutting degree, surface undulation, and erosion rate, with correlation coefficients of 0.46, 0.75, 0.82, 0.87, and 0.82, respectively. In all four quarters, the erosion rate of the gully slope and topographical factors were correlated. Erosion and topographical factors interacted with each other, and temperature and wind speed had a strong effect on the erosion rate of the gully slope and topographical factors. The relationship between surface roughness and other factors was strong. Therefore, surface roughness can be used as the best topographical factor for gully slope soil erosion in the Pisha sandstone area.

The influence of the related factors on the erosion rate and the correlation between factors was further explored on the basis of the above analysis. Given that the relationship among rainfall, solar radiation, and other related factors was weak, it was excluded from the prediction. The path analysis was performed using R and Amos software programs, and the results are shown in Figure 8. The path analysis can reflect the importance of causal traits in relation to target traits. The direct path coefficients of surface roughness, surface relief, surface cutting degree, and microslope for erosion rate were 0.721, 0.263, 0.382, and 0.216, respectively. Surface roughness, surface relief, and microslope were positively correlated with the erosion rate. Among indirect path coefficients, those of air temperature and wind speed for surface roughness were the largest, with values of −0.916 and −0.683, respectively. Air temperature and wind speed affect the erosion rate by affecting surface roughness.

4 Discussion

4.1 Effect of seasonal variation on the erosion rates of Pisha sandstone gully slopes

Seasonal climate change will increase erosion in many parts of the world and decrease human wellbeing. In this study, the changes in gully slope erosion as a result of meteorological factors were analyzed during four quarters. In each quarter, temperature (Xu et al., 2019), wind speed (Sirjani et al., 2019), rainfall (Wang et al., 2018), and solar radiation (Liu et al., 2018) were important factors affecting gully slope erosion. In the first and fourth quarters, temperature and wind speed had a greater effect on the gully slope erosion rate than other factors. The correlation coefficients of wind speed and erosion rate were 0.67 and 0.93, respectively, and those of temperature and erosion rate were 0.75 and 0.82, respectively. Therefore, consistent with the conclusion of this study, temperature and wind speed are the main factors influencing the erosion rate (Zhao et al., 2020). This study found that erosion rates were fastest in the first and fourth quarters, with values of 0.2613 and 0.2241 $t/m^2 \cdot m$, respectively, and the corresponding quarter had the lowest temperature. Average erosion rates increased with the decrease in temperature, whereas erosion rates showed the opposite trend in the second and third

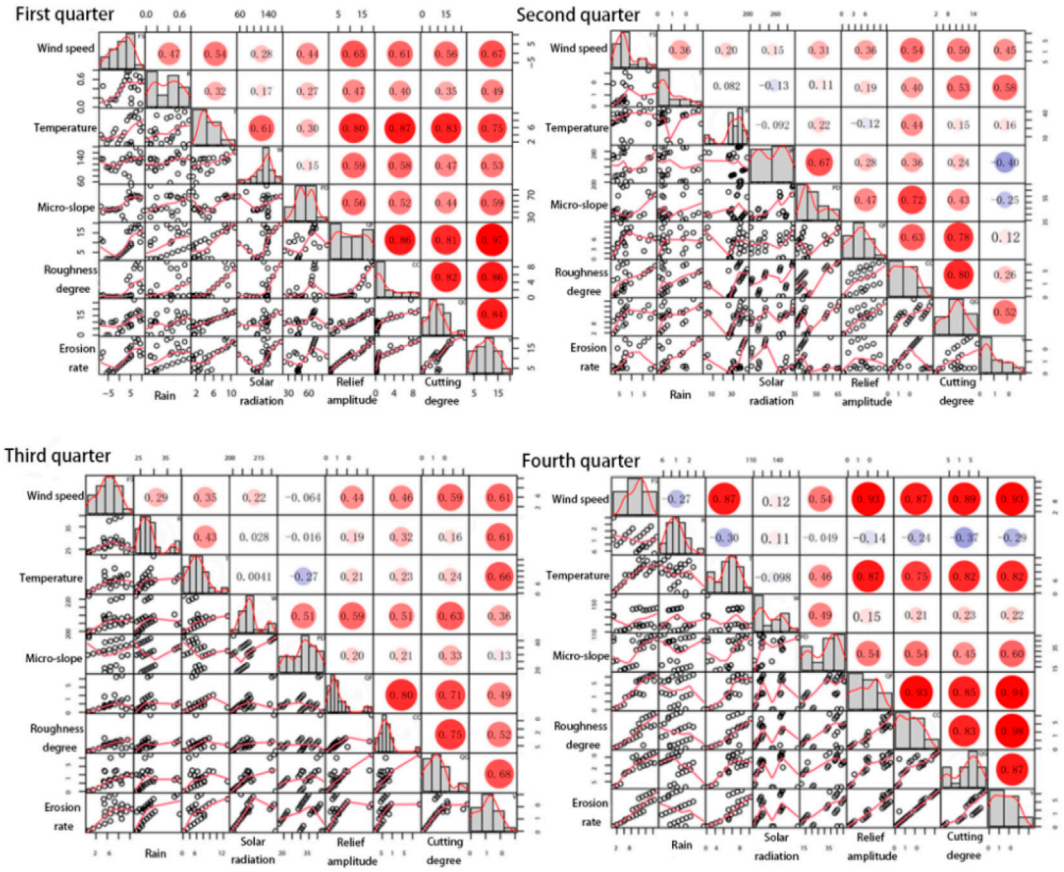

FIGURE 7
Correlation between quarterly erosion rates and slope microtopography.

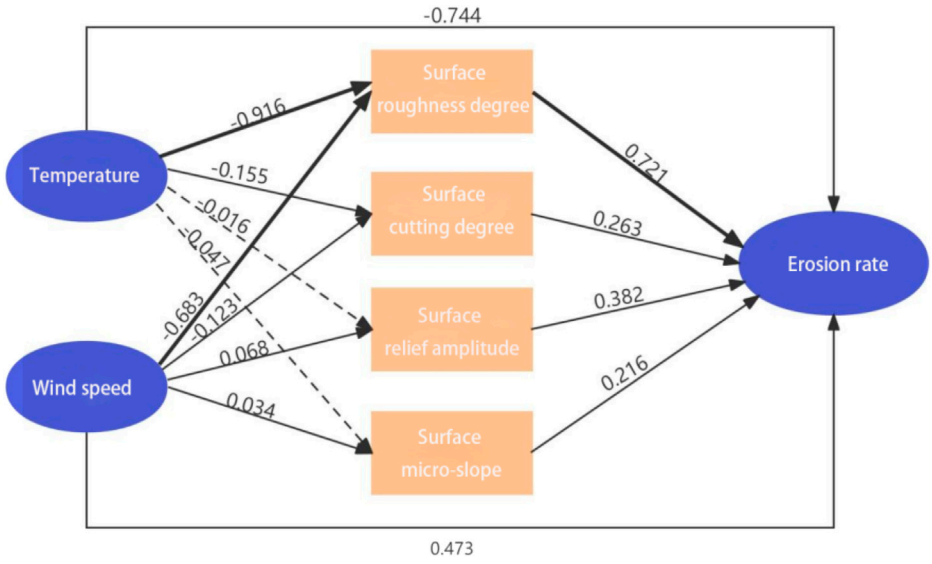

FIGURE 8
Path analysis results of the main influencing factors of the erosion rate.

quarters because the study area has a temperate continental monsoon climate. The first and fourth quarters had a broad daily temperature range and average temperatures of 0.11°C and 4.74°C, respectively. Moreover, the study area was cold and dry in winter and spring, resulting in the freezing and thawing of the soil containing a certain amount of water in the gully slope. When liquid soil becomes solid, its volume increases by approximately 90%. During water freezing, pressure is generated on the soil on both sides of cracks (Zhang et al., 2021). Therefore, in the first and fourth quarters, the erosion rates of the gully slope accelerated.

In the first and fourth quarters, the erosion intensity of the gully slope was strong, with erosion areas of 65% and 58%, respectively, which were classified as strong erosion because of the effect of wind speed, the driving force of soil erosion, and sand flow. The strength of the effect of wind speed on gully slope erosion depends first on the magnitude of wind speed (Zhou et al., 2020). Vorticity and, thus, the rate of gully slope erosion increase as wind speed increases. In this work, the first and fourth quarters had the highest wind speeds of 1.62 and 5.17 m/s, respectively, which blew away and transported soil on the gully slope. As a result of this situation, the air masses in the first and fourth quarters became unstable, warming the continent and causing low pressure. Therefore, cyclones were frequent during these two seasons. Wind speed increased during these two quarters, leading to higher amounts of erosion and deposition increased, which resulted in the fastest erosion rate. Soil erosion is one of the most urgent problems that human beings will face in the next few decades (C. Castillo and Gómez, 2016). After erosion, the deposits in the coarse sand and sandy areas of the Yellow River are continuously transported to gullies. Therefore, identifying the effect of climate change on the erosive environment in many parts of the world is necessary.

4.2 Influence of quarterly changes on microtopographical variations in Pisha sandstone gully slopes

In recent years, research methods related to gravity erosion on gully slopes have been developed mainly from actual field observations (Cao et al., 2015), indoor model tests (Chai et al., 2019), numerical simulation tests (Li et al., 2021), and other methods. With the progress of science and technology, a series of non-contact, high-precision measurement technologies have been gradually applied in the field of gravity erosion research, such as three-dimensional laser scanning (Chen et al., 2014), field layout needle measuring (Gao et al., 2021), and remote sensing image technology (Derbyshire et al., 1995). Based on the research background of the exposed Pisha sandstone, the study used field monitoring, a 3D laser scanner, and ArcGIS to monitor the changes in the slope.

The microtopographical fluctuations in the gully slopes were affected by the comprehensive responses of temperature, wind speed, precipitation, and solar radiation. As a result of the different climates in each quarter, the spatial distribution of microtopographical factors differed. With the continuous breakage of soil and rock masses, erosion per unit area decreased from 0.0871 to 0.0747 from the first to the fourth quarter, the gully slope smoothened, and the terrain factor became gentle. These effects reduced the surface roughness from 2.6906 in the first quarter to 1.7189 in the fourth quarter. This result was obtained because the average temperature in the first quarter was 44.09% higher than that in the fourth quarter. After the soil on the gully slope thawed, the meltwater increased soil moisture. This effect, in turn, sharply increased the possibility of soil erosion. After seasonal rainfall in the second and third quarters, the surface roughness of the gully slope decreased due to compaction by raindrops. This result was similar to previously reported findings (Zhang et al., 2012; Qian et al., 2021).

The changes in the four microgeomorphological factors revealed that topographic factors showed a certain degree of reduction in the second and third quarters. The surface cutting degree in the second quarter was 12.9% lower than that in the first quarter, and the surface cutting degree in the fourth quarter was 25.6% higher than that in the third quarter as a result of the seasonal rainfall that occurred in the second and third quarters. Seasonal rainfall increases the runoff of gully slopes, dissolves and softens the soil, causes the rock debris of gully slopes to disintegrate and disperse, and deposits in gentle or low-lying areas, resulting in different changes in surface cutting degrees (Qin, 2014). In the first and fourth quarters, surface undulation increased with the increase in wind speed. The loose sediment of gully slopes or the weathering product (sand material) on the bedrock is blown away due to the dynamic pressure of the wind such that gully slopes are destroyed. High wind speeds are associated with strong surface undulation. The microslope is the angle between tangent and horizontal planes passing through a point. It is essentially a function of the elevation change rate of the surface function $z = f(x, y)$ in different directions. The fitting surface method was used to extract the gully slope and generate the microslope raster data. This study found that in each quarter, erosion was intense in the upper part of the slope top. With the increase in slope, the amount of gully erosion also increased. This finding was consistent with most other previously reported results (Wang, 2019). The microslope was high in the first and fourth quarters. Given the low temperature and high snowfall in these two quarters, the slope of the gully increased such that the sliding of snow was facilitated and slip erosion occurred. In the second and third quarters, the temperature gradually increases, reducing the slope of the gully. The results showed that meteorological factors have a strong influence on microtopography. Although erosion management in the northern arid area has achieved results, the coarse sandy areas of the Yellow River may still experience degradation. Therefore, the spatial changes in microtopography must be studied to understand the environmental processes of erosion.

4.3 Relationship between meteorological factors in different quarters and gully erosion rates and microtopography

The influence of quarterly changes on gully slope microgeomorphology is mainly reflected by meteorological factors, such as temperature, wind speed, precipitation, and solar radiation. These changes indirectly affect microgeomorphological factors, such as surface roughness, surface undulation, surface cutting degree, microslope, slip erosion, and soil deposition. The

combined results of this study revealed that the correlation between the erosion rate and surface roughness was strongest in the fourth quarter with a correlation coefficient of 0.98 because snowfall occurred in the fourth quarter, and ice and snow had a high albedo under solar radiation. After solar radiation was reflected numerous times, albedo decreased in areas where surface roughness increased (Xiao et al., 2011). A strong correlation existed among wind speed, temperature, and debris slide erosion in the Pisha sandstone area. Therefore, wind speed and air temperature were set as the dominant factors in path analysis, and the direct path coefficient of surface roughness for erosion rates exceeded 0.5. This result indicated an intense promoting effect that was strongest under the promoting effect of air temperature. This factor had an indirect path coefficient of −0.916. When the heat on the surface of the slope diffuses to the atmosphere, heat transfer decelerates and temperature decreases; this effect promotes atmospheric turbulence (Feng et al., 2012), which increases slope roughness. The absolute values of the direct path coefficient of each microgeomorphological factor followed the descending order of surface roughness, surface undulation, surface cutting degree, and microslope. The indirect path coefficient of wind speed for surface undulation was 0.068, and the direct path coefficient of surface undulation for erosion rate was 0.382. Friction resistance increased as a result of high wind speeds, increasing the surface undulation of slopes (Wang and Liu, 2019) and accelerating erosion.

Research has shown that microgeomorphological factors can be used to estimate the extent of gully erosion. During ooze, a correlation exists between the erosion rates of gully slopes and changes in microgeomorphology (Li et al., 2019). Among the selected topographical factors, surface roughness had a highly significant correlation with other factors and erosion rate and can be used as the best topographical factor for evaluating gully soil erosion (Zhao et al., 2018). Therefore, the erosion rates of gully slopes in different seasons are closely related to the change in microtopography.

5 Conclusion

Based on long-term field location monitoring, the study analyzed the variation in erosion by 3D laser modeling (MDEM). The survey mainly found that in the first and fourth quarters, temperature and wind speed are the main factors influencing the erosion rate. The relationship between surface roughness on the microslope and other form factors is obvious, making surface roughness the best topographic factor for assessing slope erosion in the Pisha sandstone area. The results aim to provide a theoretical reference for understanding the process of erosion of the gully slope in the Pisha sandstone area, reveal the evolution law of erosion, and contribute to the high-quality development of the Yellow River Basin. The main conclusions are as follows:

(1) In all four quarters, gully slope erosion was dominated by strong erosion, and the first and fourth quarters had a significant influence on gully slope erosion. The erosion rates in the first and fourth quarters were 0.2634 and 0.2242 t/m^2·m, respectively. The erosion area was the largest in the first quarter and the smallest in the third quarter, with 65% and 42%, respectively.

(2) The fluctuation in erosion at the top of the gully slope in the four quarters was the most intense, followed by that at the middle of the gully slope, and that at the bottom of the gully slope showed low intensity. In the fourth quarter, surface roughness had a great influence on the erosion rate, with a correlation coefficient of 0.98. Analysis revealed that in the fourth quarter, the albedo of solar radiation decreased under the effect of snowfall, increasing surface roughness.

(3) Temperature can promote gully slope erosion, and its path coefficient was −0.744. The survey found a strong correlation between the erosion rate and surface roughness in the fourth quarter, with a correlation coefficient of 0.98. Under seasonal climate change, soil experienced freezing and thawing such that its volume increased by approximately 90%. This phenomenon generated pressure on the soil on both sides of the crack, accelerating the erosion rate.

Data availability statement

The raw data supporting the conclusion of this article will be made available by the authors, without undue reservation.

Author contributions

YZ: writing–original draft. LoL: writing–review and editing. LiL: writing–review and editing. SZ: writing–review and editing. WZ: writing–review and editing. YR: writing–review and editing. YY: writing–review and editing.

Funding

The author(s) declare that financial support was received for the research, authorship, and/or publication of this article. National Nature Fund 2022 NSF-Spatial and Temporal Variability of Erosion on Arsenic Sandstone Slopes and Interfeedback Mechanisms for the Evolution of Vegetation Patch Patterns.

Conflict of interest

The authors declare that the research was conducted in the absence of any commercial or financial relationships that could be construed as a potential conflict of interest.

Publisher's note

References

Barnes, N., and Luffman, N. (2016). "Gully erosion and freeze-thaw processes in clay-rich soils," in *Northeast Tennessee*. USA: GeoResJ.

Bi, S., Yuan, C., Liu, C., Cheng, J., Wang, W., and Cai, Y. (2021). A survey of low-cost 3D laser scanning technology. *Appl. Sci.* 11 (9), 3938. doi:10.3390/app11093938

Cao, B., Jiao, J., Wang, Z., Wei, W., and Li, Y. (2015). Landslide characteristics under heavy rain in yan River Basin in 2013. *Res. Soil Water Conservation* 22 (6), 103–109. doi:10.13869/j.cnki.rswc.20151116.015

Castillo, C., and Gómez, J. A. (2016). A century of gully erosion research: Urgency,complexity and s tudy approaches. *Earth Sci. Rev.* 160, 300–319. doi:10.1016/j.earscirev.2016.07.009

Chai, Y., Zhou, B., Lu, W., and Wu, Y. (2019). Erosion process and infiltration characteristics of red clay slope deposits in lagoon under simulated rainfall conditions. *Water Soil Conservation Sci. China* 17 (01), 10–15. doi:10.16843/j.sswc.2019.01.002

Chen, Z., Tingwu, L., Yan, Q., Hu, H., Xiong, M., and Li, Z. (2014). Calculation method of erosion on the slope of landslide accumulation body in Wenchuan earthquake area. *J. Agric. Mach.* 45 (4), 195–200. doi:10.6041/j.issn.1000-1298.2014.04.031

Chen, S., Xiaoli, L., Qiang, Z., and Mingyu, L. (2016). Deformation characteristics of Ordos red arsenic sandstonein freeze-thaw cycle. *China Natl. Sci. Soil Water Conservation* 14 (04), 34–41. doi:10.16843/j.sswc.2016.04.005

Cndido, B. M., James, M., Quinton, J., de Lima, W., and Naves Silva, M. L. (2020). Sediment source and volume of soil erosion in a gully system using UAV photogrammetry. *Rev. Bras. Cienc. do Solo*. doi:10.36783/18069657rbcs20200076

Derbyshire, E., Van Asch, T., Billard, A., and Meng, X. (1995). Modelling the erosional susceptibility of landslide catchments in thick loess: Chinese variations on a theme by Jan de Ploey. *Catena* 25 (1-4), 315–331. doi:10.1016/0341-8162(95)00015-k

Du He, Q., Tao, W., and Xian, X. (2017). Potential wind erosion rate response to climate and landuse changes in the watershed of the Ningxia–Inner Mongolia reach of the Yellow River,China,1986–2013. *Earth Surf. Process. Landf.* 42 (13), 19 23–1937. doi:10.1002/esp.4146

Fang, H. Y., and Guo, M. (2015). Aspect-induced differences in soil erosion intensity in a gullied hilly region on the Chinese Loess plateau. *Environ. Earth Sci.* 74 (7), 5677–5685. doi:10.1007/s12665-015-4648-4

Feng, J. W., Liu, H. Z., Wang, L., Qun, D., and Liqing, S. (2012). Variation characteristics of surface roughnes and turbulent flux of different underlying surfaces in semi-arid region. *Sci. China:Earth Sci.* 42 (01), 24–33. doi:10.1360/zd-2012-42-1-24

Gao, J., Qisen, A., Han, L., Gao, L., Lei, Y., Ma, S., et al. (2021). 20172018 Yellow earth mound Data set of gravity erosion observations in Xindiangou Basin, the first sub-area of Linggully area. *Chin. Sci. Data (China UKOnline version)* 6 (03), 113–120. doi:10.12072/ncdc.HWSDZhan.db0051.2020

Gao, C., Yao, S., Pengfei, L., and Mu, X. (2020). Progress of gravity erosion on the Loess Plateau. *People's YellowRiver* 42 (06), 99–195. doi:10.3969/issn.1000-1379.2020.06.020

Guo, J. W., Qi, Y., Zhang, L., Zheng, J., Sun, J., Tang, Y., et al. (2024). Identifying and mapping the spatial factors that control soil erosion changes in the Yellow River Basin of China. *Land* 13 (3), 344. doi:10.3390/land13030344

Li, L., Qin, F. C., and Yao, X. L. (2021). Relationship between the slope microtopography and the spatial redistribution pattern of soil organic carbon under water erosion. *J. Soil and Water Conservation* (5), 76. doi:10.2489/JSWC.2021.02144

Li, M. T., Nie, J., Li, Z., Pullen, A., Abell, J. T., Zhang, H., et al. (2023). A middle Pleistocene to Holocene perspective on sediment sources for the Tengger Desert,China. *Catena* 228, 107119. doi:10.1016/j.catena.2023.107119

Li, Q. X., Ding, W. F., Zhu, X. D., and Pang, Y. (2019). Effects of rainfall in tensity and surface roughness on microtopography and erosion of gully slopes. *J. Yangtze River Acad. Sci.* 36 (01), 41–47. doi:10.11988/ckyyb.20170619

Li, Y. S., Jia, X., Wang, H., and Ma, Q. (2023). Desert river channel deposition characteristics and their implications for lateral infusion of aeolian sand in the Ulan Buh desert reaches of the Yellow River. *Environ. Earth Sci.* 82 (22), 525. doi:10.1007/s12665-023-11224-3

Li, Z. Y., and H, Y. F. (2016). Impacts of climate change on water eros-ion:A review. *Earth-Science Rev.* 163, 94–117. doi:10.1016/j.earscirev.2016.10.004

Liu, F., Chen, L., Zhang, B., Wang, G., Qin, S., and Yang, Y. (2018). Ultraviolet radiation rather than inorganic nitrogen inc reases dissolved organic carbon biodegradability in a typical thermo-erosion gully on the Tibetan Plateau. *Sci. Total Environ.* 627 (JUN.15), 1276–1284. doi:10.1016/j.scitotenv.2018.01.275

Liu, W., Song, X., Luo, J., and Hu, L. (2020). The processes and mechanisms of collapsing erosion for granite residual soil in southern China. *J. soil and sediments* 20 (2), 992–1002. doi:10.1007/s11368-019-02467-4

Liu, Y., Cheng, J., and Zhang, Y. (2024). Nonlinear response of soil erosion to climate change and ecological policies on the Tibetan Plateau. *Soil Water Conservation Res.* 31 (04), 126–134. doi:10.13869/j.cnki.rswc.2024.04.044

Liu, Y., Gao, G., Li, H., Liu, L., Fan, Z., and Wen, T. (2022). Spatiotemporal variations and causes of wind/rainfall erosion climatic erosivity in Qinghai Province, China. *Atmosphere* 13 (10), 1649. doi:10.3390/atmos13101649

Lyu, L., Wang, Z., Cui, P., and Xu, M. (2017). The role of bank erosion on the initiation and motion of gully debris flows. *Geomorphology* 285, 137–151. doi:10.1016/j.geomorph.2017.02.008

Ma, Z. (2020). *Characterization and regulation of soil moisture under typical degraded vegetation in overlyingthe Pisha sandstone area [D]*. Shaanxi: Northwest Agriculture and Forestry University.

Matsunaga, K., and Zhimao, G. (2007). Analysis of geomorphological factors of gravity erosion on the Loess Plateau--Regional characteristics from the scale frequency of occurrence. *Soil Water Conservation Bull.* (1), 55–57+91. doi:10.13961/j.cnki.stbctb.2007.01.013

Mostafa, A. B. (2015). Ebrahim.3D laser scanners techniques overview. *Int. Jour nal Sci. Res.* 4 (10), 5–611.

Ni, J. R., Li, X. X., and Borthwick, A. G. L. (2008). Soil erosion assessment based on minimum Polygons in the Yellow River basin,China. *Geomorphology* 93 (3-4), 233–252. doi:10.1016/j.geomorph.2007.02.015

Qian, Q. Y., Qin, F. C., Li, L., Yang, Z., and Zhang, R. (2021). Spatial heterogeneity of surface roughness of gully slope erosion under natural rainfall conditions. *J. Soil Water Conser vation* 35 (03), 46–52. doi:10.13870/j.cnki.stbcxb.2021.03.007

Qin, F. (2014). *Characteristics of surface microtopography change in purple soil are and its influence on soil erosion[D]*. Sichuan, China: Sichuan Agricultural University (SACU).

Ryan, L., Kate, M., and Jacobus, J. (2021). An interrogation of research on the influence of rain fall on gully erosion. *Catena* 206, 105482. doi:10.1016/j.catena.2021.105482

Sirjani, E., Sameni, A., Moosavi, A. A., Mahmoodabadi, M., and Laurent, B. (2019). *Portable wind tunnel experiments to study soil erosion by wind and its link to soil properties in the Fars province,Iran*. Elsevier.

Valjarević, A., Srećković-Batoćanin, D., Živković, D., and Perić, M. (2015). GIS analysis of dissipation time of landscape in the Devil's city (Serbia). *Acta Montan. Slovaca* 20 (2). doi:10.3390/ams20020148

Wang, J., Zhong, L., and Zhao, W. (2018). The influence of rainfall and landuse patterns on soil erosion in multi-scale watersheds:A case study in the hilly and gully are on the Loess Plateau. *China* 28 (10), 12. doi:10.1007/s11442-018-1553-2

Wang, W. W. (2019). *Soil erosion evolution characteristic of purple soil slope cultivated land under different slopes[D]*. Sichuan, China: Sichuan Agricultural University (SACU).

Wang, X. S., and Liu, L. (2019). Research on topographical relief and its relationship with wind speed in Yunnan Province based on SRTM DEM data. *Gansu Sci. J.* 31 (06), 30–35+67. doi:10.16468/j.cnki.issn1004-0366.2019.06.006

Wang, W., Chen, X., Xiaoqian, L., Jianying, G. O., Jinrong, L., Zhang, T., et al. (2019). Characteristics and prediction of spatial and temporal distribution of sand production by rainfall erosion in Ten Kongtui. *People's Yellow River* 41 (04), 1–6+10.

Wen-Yi, Y., Chang-Ming, L., Pan, Z., and Won-Chang, W. (2018). Research and prospect of erosion mechanism of arsenic sandstone. *People's Yellow River* 40 (06), 1–7+65. doi:10.3969/j.issn.1000-1379.2018.06.001

Wulf, O., and Wagner, B., Fast 3D scanning methods for laser measurement systems. 2003.

Wu, Y. (2020). "Research on physicochemical characteristics and erosion mechanism of arsenic sandstone in the middle reach of the Yellow River and integration and demonstration of binary management model," in *Small watersheds and demonstration [D]* (Beijing: China University of Geosciences).

Xiao, D. P., Tao, F. L., and Moiwo Juana, P. (2011). Research progress on surface albedo under global change. *Adv. Earth Sci.* 26 (11), 1217–1224. doi:10.11867/j.issn.1001-8166.2011.11.1217

Xu, J., Jin, Z., Liu, X., Hu, W., Yang, Q., Hao, Y., et al. (2019). Gully erosion induced by snowmelt in Northeast China: a case st udy. *Sustainability* 11 (7), 2088. doi:10.3390/su11072088

Yan, W., Yang, Z., Liu, H., Cai, H., and Min, W. (2016). Material composition ofthe Pisha sandstone and its effect on nutrient content. *People's Yellow River* 38 (06), 18–21+25. doi:10.3969/j.issn.1000-1379.2016.06.005

Yang, Z. Q., Qin, F. C., Li, L., Ren, X., Qian, Q., and Han, J. (2019). Spatial distribution characteristics of soil organic matter and its influencing factors in small watershed of feldspathic sandsto neregion. *Trans. Chin. Soc. Agric.* 201935 (17), 154–161.

Ye, H., Jian-Sheng, S., Hou, H., Ying-Chun, S., Yan-Pei, C., and Jiao, G. (2008). Influence of lithologic characteristics of the Pisha sandstones in southern Inner Mongolia on gravity erosion. *Arid Zone Res.* (03), 402–405. doi:10.13866/j.azr.2008.03.023

Ye, H., Jian-Sheng, S. H. I., Xiang-Quan, L. I., Hong-Bing, H. O. U., Ying-Chun, S. H. I., and Yan-Pei, CHENG.(2007) Analysis of the effect of lithological characteristics ofthe Pisha sandstone on erosionresistance.

Yousefi, S., Jaafari, A., Valjarević, A., Gomez, C., and Keesstra, S. (2022). Vulnerability assessment of road networks to landslide hazards in a dry-mountainous region. *Environ. Earth Sci.* 81, 521. doi:10.1007/s12665-022-10650-z

Yu, B., Wang, T., and Zhu, Y. (2016). Topographical and rainfall factors determining the formation of gully-type debris fllows caused by shallow landslides in the Day area, Guizhou Province, China. *Environ. Earth Sci.* 75 (7), 1–18. doi:10.14042/j.cnki.32.1309.2016.04.008

Yuhong, L. (2018). Study on the physical properties of water in lagoon eroded soils of loess residual plateau area. *People's Yellow River* 40 (08), 96–98+119.

Yujie, L. (2021). *Study on the mechanism of loess slope erosion in the Yellow River desert basin based on mutation theory*. orchid State Polytechnic University. [D].

Zhang, L., Ren, F., Li, H., Cheng, D., and Sun, B. (2021). The influence mechanism of freeze-thaw on soil erosion: a review. *Water* 202 (8). doi:10.3390/w13081010

Zhang, Y., Feihang, S., Zhang, Y., Min, L., Guoyi, C., and Zhengze, L. (2023). Spatial and temporal changes and driving factors of soil erosion in the middle reaches of the Yellow River. *Soil Water Conservation Res.* 30 (05), 1–12. doi:10.13869/j.cnki.rswc.2023.05.003

Zhang, X., Wei, C. F., Ni, J. P., and Zhang, S. (2012). Study on the relationship between rural settlement distribution and geomorphological elements in karst trough valley area of C hongqing. *Karst China* 31 (01), 59–66. doi:10.3969/j.issn.1001-4810.2012.01.011

Zhang, Z., and Kai, X. (2021). Ecological management strategy of soil erosion and geohazardsin Longdong Loess Plateau. *Undergr. Water* 43 (05), 222–225+283. doi:10.19807/j.cnki.DXS.2021-05-078

Zhao, C., Zhang, H., Wang, M., Jiang, H., Peng, J., and Wang, Y.Jiang Hong, PengJian , WangYanglin (2020). Impacts of climate change on wind erosion in southern Africa between 1991 a2015.

Zhao, S. Q., Wang, X. H., Shu, T. Z., and Tang, R. (2018). Study on topographical factors of soil erosion at the regional scale in karst region. *Arid Land Resour. Environ.* 32 (05), 97–103. doi:10.13448/j.cnki.jalre.2018.147

Zhou, C. L., Yang, F., Mamtimin, A., Huo, W., Liu, X., He, Q., et al. (2020). Wind erosion events at different wind speed levels in the Tarim Basin. *Geomorphology* 369, 107386. doi:10.1016/j.geomorph.2020.107386

Zhu, B., Zhou, Z., and Li, Z. (2021). Soil erosion and controls in the slope-gully system of the Loess Plateau of China:A review. *Front. Environ. Sci.* 9. doi:10.3389/fenvs.2021.657030

Zhu, J., Chen, Z., and Zhu, Y. (2017). Distribution pattern and development characteristics of landslides in Yan'an. *Geoscience Technol. Situat. News* 36 (02), 236–243.

Zhu, X., Zhang, L., and Yang, S. (2019). Analysis of spatial and temporal patterns of rainfall-induced loess landslides in Lanzhou and critical rainfall volume prediction. *Chin. J. Geol. Hazards Prev.* 30 (04), 24–31. doi:10.16031/j.cnki.issn.1003-8035.2019.04.04

Zou, Z., Tao, Y., Gao, Y., Liu, Z., Li, W., Tian, Z., et al. (2023). Soil moisture dynamics near a gully head in relation to the trigger of collapse in granite red soil slope in southern China. *Geomorphology* 420, 108493. doi:10.1016/j.geomorph.2022.108493